2C4-4

SAR Calculations in Various Parts of Pregnant Woman during MR Imaging

#Satoru Kikuchi [1], Kazuyuki Saito [2], Masaharu Takahashi [2],
Koichi Ito [3], and Hiroo Ikehira [4]
[1] Graduate School of Science and Technology, Chiba University
[2] Research Center for Frontier Medical Engineering, Chiba University
[3] Faculty of Engineering, Chiba University
1-33 Yayoi-cho, Inage-ku, Chiba 263-8522, [1]kikuchi@graduate.chiba-u.jp
[4] National Institute of Radiological Sciences
4-9-1 Anagawa, Inage-ku, Chiba 263-8555, Japan

1. Introduction

Magnetic resonance imaging (MRI) is one of effective diagnostic modalities without using ionization radiation. The MRI system is composed of several units including radio frequency (RF) technologies, and RF coil is one of the important units for imaging. The RF coil operates as an antenna, which "radiates the RF pulses to the body" and "receives the nuclear magnetic resonance (NMR) signals emitted from the body". Here, according to shape of the RF pulses, various types of images inside the human body can be obtained. Figure 1 shows the one type of RF pulses. In general, although widths of pulses are narrow, their amplitudes are not so low. Therefore, it is necessary to assess the specific absorption rate (SAR) in the human body due to the radiated RF pulse from the RF coils. Until now, the estimation of SAR in the human head has been studied during MR imaging [2], [3]. However, in recent years, MR imaging is used not only for the head but also for other parts of the body. Especially, in this study, the SAR distributions in the abdomen of a pregnant woman are investigated. In general, an ultrasound diagnostic system is used for the medical examination of the pregnant woman. However, the MR imaging is sometimes chosen for the medical reasons. Therefore, it is important to investigate the SAR in the pregnant woman and her fetus [4], [5]. Concretely, we assumed the imaging of a pregnant woman in early period and in her 28th gestational week. In this study, the finite-difference time-domain (FDTD) calculations are employed and two types of realistic woman models as previously developed are adapted for the SAR calculations. Moreover, various position of the RF coil to the SAR inside the fetus is investigated.

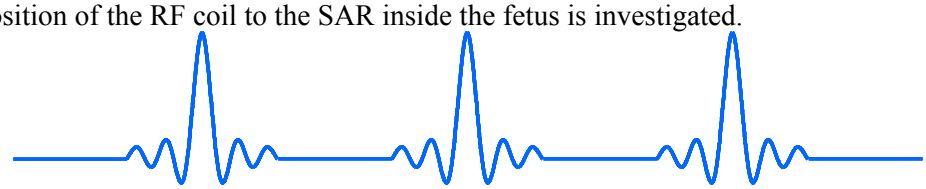

Figure 1: Type of RF pulses

2. Calculation Models

2.1 Realistic Woman Models

Figures 1 (a) and (b) show the two types of woman models for the FDTD calculations. Here, the realistic high-resolution whole-body voxel model of a Japanese female, developed at the National Institute of Information and Communications Technology (NICT), Japan [6] is used for the calculation of the pregnant woman in early period (Model A). Moreover, the 28th gestational week woman model [7], which is developed by the NICT and Chiba University, is applied as the last stage of pregnancy period (Model B). The voxel size of these models (Model A and Model B) is $2\times2\times2$ mm^3. In order to develop Model B, first, the voxel model of the fetus (including fetal body, fetal brain, fetal eyes, amniotic fluid, placenta, and uterus wall) is developed from the MR images of a pregnant woman. These images of the 28th gestational week pregnant woman volunteer were taken using a 1.5 T MRI system. Next, the abdomen of the Model A is expanded following the standard shape of the pregnant woman. Finally, these two models are combined and adjusted following the comments from medical doctors. In addition, the physical properties of these models are determined from [5], [8], [9].

ISBN: 978-4-88552-223-9 C3055©IEICE

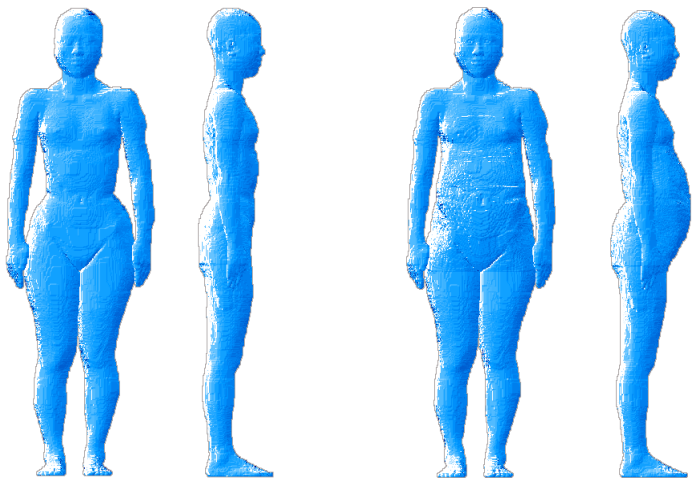

(a) Non-pregnant model (Model A) (b) Pregnant model (Model B)
Figure 1: Realistic woman models.

2.2 Numerical calculation model

In this study, a bird cage coil is employed as one of the fundamental RF coils for MRI system. The operating frequency of the coil is around 64 MHz, which is used in the 1.5 T (Tesla) MRI system. Figure 2 shows the FDTD calculation model including the pregnant woman model and the coil. This coil consists of two end rings and eight legs and RF shield whose widths are 10 mm. The diameter and the length of the bird cage coil were set as 600 and 700 mm, respectively, so that the woman model can be inserted. A cylindrical RF shield, with a diameter of 740 mm and a length of 1260 mm, has been located lateral to the coil.

Before the SAR calculations, the capacitors on the bird cage coil were adjusted so that the resonance frequency of the coil is around 64 MHz. In order to determine the capacitances, "bird cage builder", which calculates the resonant frequency of the bird cage coil by its equivalent circuit model, was employed. In order to calculate the whole body of the woman models, a large computational space was determined and a supercomputer (Hitachi SR11000) in the Institute of Media and Information Technology, Chiba University was employed. Steady state analysis is performed by feeding a sinusoidal electric field on the feeding gap to calculate the SAR distribution in the woman model.

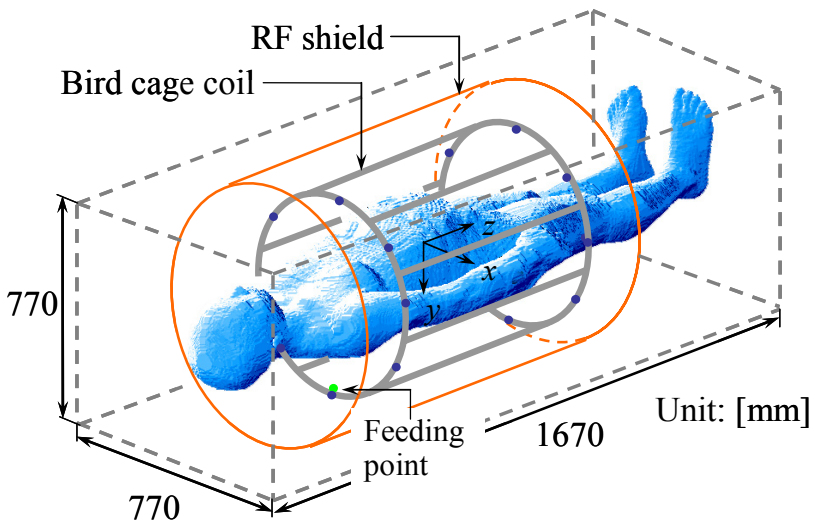

Figure 2: Numerical calculation model.

3. Calculated results

3.1 SAR distributions

Figures 3 and 4 show the calculated SAR distributions by the Models A and B, respectively. Figures 3(a) and 4(a) show the SAR distributions in the observation plane, and Figures 3(b) and 4(b) show the SAR distributions on the observation line. Here, the observation plane is the coronal plane (*xz* plane) including the uterus (for Model A), around the center of the fetus (for Model B). Moreover, positions of observation lines A-A' and B-B' are indicated in the Figures 3(a) and 4(a). Here, the SAR values are normalized by 1.0 W radiated power from the coil in both cases. In Model A, relatively high SAR values are observed around the skin, muscle, etc which have a high electrical conductivity and are located close to the surface of the maternal body. Moreover, a high SAR value is observed inside of the thigh and axillars because of the narrow gap. Meanwhile, the SAR in the uterus and the ovary are low compared with the above mentioned regions.

In Model B, relatively high SAR values are observed around the same regions as in Model A. Moreover, relatively high SAR values are observed around the border of amniotic fluid (around x =±100 mm, z =100 mm in Fig. 4(a)).

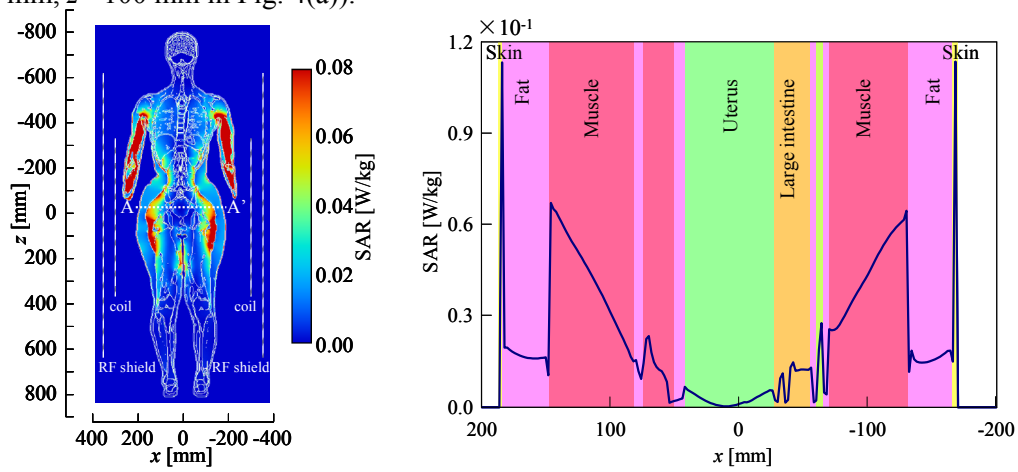

(a) Coronal plane (b) Observation line A-A'

Figure 3: Calculated SAR distribution (Model A). Normalized by 1.0 W radiation power.

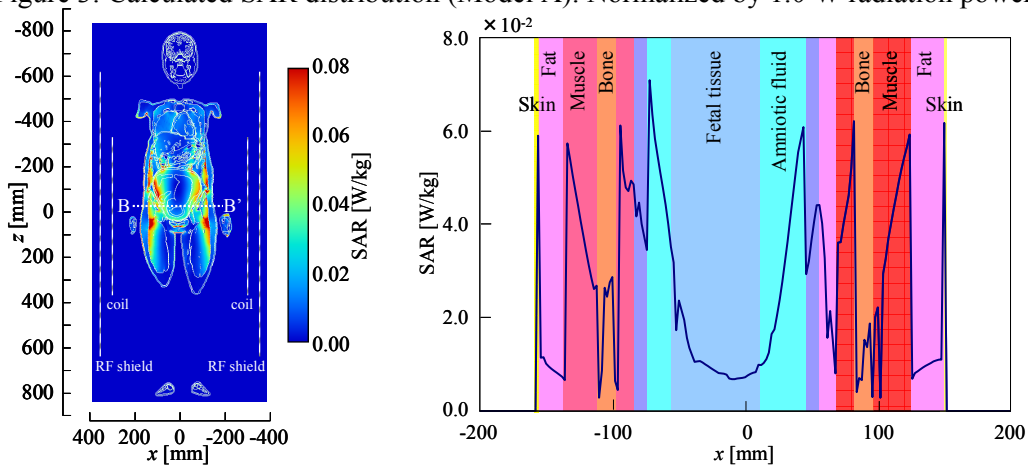

(a) Coronal plane (b) Observation line B-B'

Figure 4: Calculated SAR distribution (Model B). Normalized by 1.0 W radiation power.

3.2 Fetus average SAR under various positions of the coil

It is considered that the position of the coil is different for each imaging. Hence, the SARs in the maternal body and her fetus are calculated under various position of the coil. Concretely, the coil position will be shifted ±150 mm every 50 mm in z direction and "z =0" on horizontal axis means that the origin of coordinate system and the center of the coil are the same position. Figures 5(a) and (b) show average SAR under several positions of the coil in the Models A and B, respectively. From Fig. 5(a), the whole body average SAR is almost the same under various position of the coil. Mean-

while, the uterus and ovary average SAR show maximum values at z = 150 mm. From Fig. 5(b), the values of the whole body average SAR are observed same tendency as in Fig. 5(a). Moreover, the fetus average SAR and fetal brain average SAR show maximum values at z =100 mm.

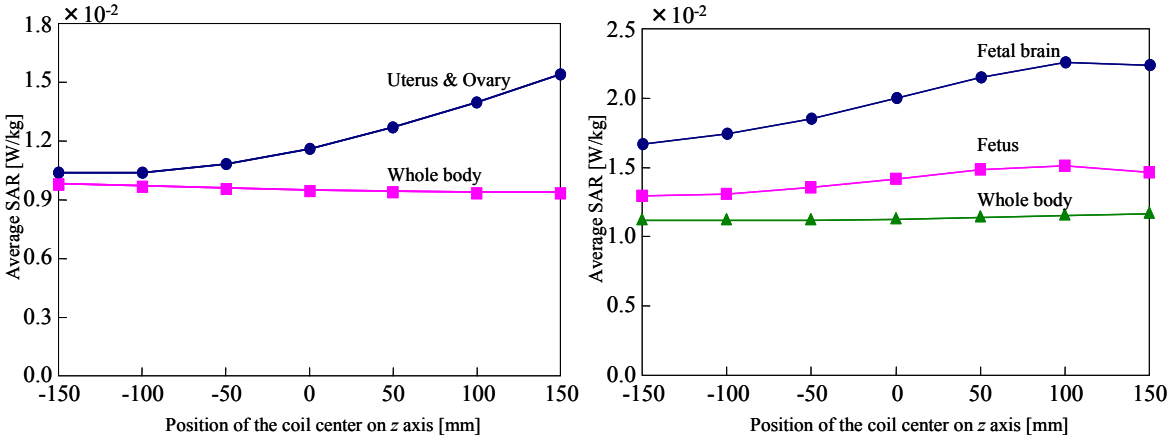

(a) Model A (b) Model B

Figure 5: Calculated average SARs under various coil positions

4. Conclusion

In this study, the SAR distributions of two types of woman models (pregnant woman in early period and 28th gestational week woman) were calculated. As a result of calculations, low SAR values were observed around the uterus (for the early period model) and the fetus (for the 28th gestational week model). Moreover, the SARs under various position of the RF coil are also calculated. As a further study, it is necessary to calculate the temperature rise inside the fetus due to the RF pulse radiation based on these results.

Acknowledgments

The authors would like to thank Dr. Tomoaki Nagaoka and Dr. Soichi Watanabe, National Institute of Information and Communications Technology, Tokyo Japan for their valuable comments in terms of using the realistic high-resolution whole-body voxel models.

References

[1] J. Jin, *Electromagnetic analysis and design in magnetic resonance imaging*, CRC Press, Boca Raton, 1998.

[2] U.D. Nguyen *et al.*, "Numerical evaluation of heating of the human head due to magnetic resonance imaging," *IEEE Trans. Biomed. Eng.*, vol. 51, no. 8, Aug. pp. 1301-1309, 2004.

[3] J. Chen *et al.*, "Numerical simulation of SAR and *B*1-field inhomogeneity of shielded RF coils loaded with the human head," *IEEE Trans. Biomed. Eng.*, vol. 45, no. 5, May pp. 650-659, 1998.

[4] J. W. Hand *et al.*, "Prediction of specific absorption rate calculations in mother and fetus associated with MRI examinations during pregnancy," *Magn. Reson. Med.*, vol. 55, pp. 883-893, 2006.

[5] D. Wu *et al.*, "Evaluations of specific absorption rate and temperature increase within pregnant female models in magnetic resonance imaging birdcage coils," *IEEE Trans. Microw. Theory Tech.*, vol. 54, no. 12, pp. 4472-4478, Dec. 2006.

[6] T. Nagaoka *et al.*, "Developpment of realistic high-resolution whole-body voxel models of Japanese adult males and females of average height and weight, and application of models to radio-frequency electromagnetic-field dosimetry," *Phy. Med. Biol.*, vol. 49, pp. 1-15, 2004.

[7] T. Nagaoka *et al.*, "An anatomically realistic voxel model of the pregnant woman and numerical dosimetry for a whole-body exposure to RF electromagnetic fields," *Proceedings of 28th IEEE EMBS Annual International Conference*, pp. 5463-5467, Sep., 2006.

[8] C. Gabriel, "Compilation of the dielectric properties of body tissues at RF and microwave frequencies," *Armstrong Laboratory, Brooks Air Force Technical Report* AL/OE-TR-1996-0037, 1996.

[9] F. A. Duck, *Physical Properties of Tissue*. New York: Academic, 1990.